ORIGINAL RESEARCH ARTICLE

Compound Heterozygous Mutations in *ZNF408* in a Patient with a Late Onset Pigmentary Retinopathy and Relatively Preserved Central Retina

Jennifer B. Nadelmann · Erin C. O'Neil · Dale S. Kim · Jane Juusola · Tomas S. Aleman

Abstract

Purpose To describe in detail the phenotype of a patient with compound heterozygous mutations in *ZNF408* and an adult-onset pigmentary retinopathy rather than familial exudative vitreoretinopathy as expected with heterozygous mutations in this gene.

Methods A 70-year-old male presented with a pigmentary retinopathy, which prompted a genetic evaluation that revealed two variants in trans in the *ZNF408* gene. He underwent an ophthalmic examination, kinetic fields, electroretinography (ERG), spectral-domain optical coherence tomography (SD-OCT), fundus autofluorescence, wide-angle fluorescein angiography and near-infrared imaging.

Results Visual acuity was 20/20 for both eyes. Fundus examination showed epiretinal membrane, vascular attenuation and peripheral bone spicule pigmentation in both eyes. Fluorescein angiography showed no vascular anomalies in both eyes. Fundus autofluorescence showed a preserved island of fundus autofluorescence centrally. Visual field by kinetic perimetry (V-4e stimulus) showed generalized constriction to 40 degrees of eccentricity and by an I-4e target showed generalized constriction to 10 degrees of eccentricity. ERG showed detectable but reduced cone-mediated responses. SD-OCT demonstrated preserved outer nuclear layer thickness centrally, which decreased with eccentricity. Static perimetry showed substantial rod and cone sensitivities centrally that declined with eccentricity. A next-generation sequencing panel revealed bi-allelic variants (p.Arg567Ter; c.1699C > T and p.Leu566His; c.1697 T > A) in the *ZNF408* gene.

Conclusions *ZNF408*-associated retinal dystrophies can present with predominantly retinal findings and should be considered in the differential diagnosis of retinitis pigmentosa. Our study revealed a novel variant p.L566H, which to our knowledge has not previously been reported.

J. B. Nadelmann · E. C. O'Neil · D. S. Kim · T. S. Aleman (✉)
Scheie Eye Institute at the Perelman Center for Advanced Medicine, Department of Ophthalmology, University of Pennsylvania, 3400 Civic Center Boulevard, Philadelphia, PA 19104, USA
e-mail: aleman@pennmedicine.upenn.edu

J. Juusola
Clinical Genomics Program, GeneDx, Gaithersburg, MD, USA

T. S. Aleman
The Center for Advanced Retinal and Ocular Therapeutics, Department of Ophthalmology, University of Pennsylvania, Philadelphia, PA, USA

Introduction

Retinitis pigmentosa (RP) is a syndromic diagnosis that includes a large group of genetically heterogeneous and phenotypically diverse, progressive inherited retinal degenerations (IRDs). Typical presentation is during in adolescence to early adulthood, with symptoms of mid-peripheral/peripheral visual field loss, particularly in dim lighting, associated with variable degrees of rod and cone photoreceptor dysfunction and with a pigmentary retinopathy on fundus examination [1–10]. The condition is classically diagnosed through an abnormal electroretinogram (ERG), visual field testing and/or by retinal imaging [1–9]. Hundreds of genetic defects have been identified in non-syndromic and syndromic forms of RP (RetNet; http://www.sph.uth.tmc.edu/retnet/, provided in the public domain by the University of Texas Houston Health Science Center, Houston, TX), mostly inherited through autosomal dominant, autosomal recessive and X-linked patterns of inheritance [1–3].

Among the latest additions to the list of molecular causes of RP are recessively inherited variants in genes that were discovered in, and are typically associated with, an infantile-onset, dominantly inherited group of early onset vasculopathies, collectively known as familial exudative vitreoretinopathy (FEVR), namely ZNF408 [11–15]. In addition to these recessive retinopathies, dominantly and recessively inherited chorioretinal degenerations have been since added to the FEVR spectrum with at least four genes entering the list (LRP5, KIF11, TUBGCP4 or TUBGCP6) [16]. The ZNF408 gene, located on chromosome 11p11.2, encodes a protein member of the zinc finger transcription factors that consists of ten zinc finger motifs of Cys2-His2 (C2H2-ZF) proteins organized in a tandem array, located near the C-terminus. The protein has a nuclear localization, is widely expressed, especially in the retina, specifically within the retinal vasculature and in both cone and rod photoreceptors, with evidence supporting a role in retinal vasculogenesis [13, 17, 18].

In this study we describe in detail the phenotype of a patient diagnosed with RP in whom novel compound heterozygous missense variants in ZNF408 were identified, adding support to the expanded spectrum of disease expression associated with variants in this gene.

Methods

This is a retrospective review of the clinical record of a patient seen as part of his standard of care. The visit adhered to HIPAA regulations, the patient offered informed consent to the diagnostic procedures and all personal identifiers have been removed. The patient underwent a complete ophthalmic examination, Goldmann kinetic fields and Farnsworth D-15 color vision testing. Wide-angle (200°) fundus imaging was performed using a scanning laser system (Optos Inc. Marlborough, MA). Spectral-domain optical coherence tomography (SD-OCT) imaging, en-face near-infrared (NIR) reflectance (REF) and fundus autofluorescence (FAF) imaging were performed using a Spectralis-HRA system (Heidelberg Engineering GmbH, Heidelberg, Germany). Segmentation of the SD-OCT was performed with Image J analysis software [available in the public domain at https://imagej.nih.gov/ij/download.html]. Achromatic and chromatic (500 nm and 650 nm) static perimetry was performed using a modified Humphrey Field Analyzer (HFA II-I, Carl Zeiss Meditec, Dublin, CA), following published methodology [8, 19]. Thresholds were measured along the horizontal meridian at 2° intervals, extending to 30° of eccentricity, corresponding to the retinal region scanned with SD-OCT as detailed above. Standard full-field electroretinograms (ERGs) were recorded using a computer-based system (Espion, Diagnosys LLC, Littleton, MA) [20]. Dark-adapted rod-mediated responses (DA 0.01 protocol) were elicited with a dim white flash (0.01 cd.s.m^2); dark-adapted mixed cone-rod responses (DA 3.0) were elicited with a standard flash (3.0 cd.s.m^2); light-adapted cone-mediated responses were elicited with the same stimulus in response to 1 Hz stimulation or a 30 Hz flicker.

The patient underwent proband-only Retinal Dystrophy Xpanded panel testing at GeneDx (Gaithersburg, MD, USA). The test utilizes exome capture, next-generation sequencing, Sanger sequencing of specific regions and targeted analysis of a comprehensive list of approximately 780 genes currently associated with retinal dystrophy. Using genomic DNA from the proband, the exonic regions and flanking splice junctions of the genome were captured using the IDT xGen Exome Research Panel v1.0 (Integrated DNA Technologies, Coralville, IA). Massively parallel (NextGen) sequencing was done on an

Illumina system with 100 bp or greater paired-end reads. Reads were aligned to human genome build GRCh37/UCSC hg19 and analyzed for sequence variants using a custom-developed analysis tool. Additional sequencing technology and variant interpretation has been previously described [21].

Results

A 70-year-old male presented to our clinic for evaluation of a pigmentary retinopathy. He had been visually asymptomatic until 2013, when, at age 65, he noted a visual field defect as objects would suddenly appear in his field of vision, and he would bump his head on overhead objects. He had a history of HLA-B27 positive bilateral anterior uveitis diagnosed in his 40 s, which resolved with short-term (< 3 months) administration of topical steroids leaving no sequelae. During a fundus examination during a new uveitis flare in the left eye at age 69, pigmentary changes were noted in the peripheral retina, prompting further evaluation. He was otherwise healthy with the exception of osteoarthritis of the knee requiring bilateral knee replacements at age 65, mild hypertension and hypercholesterolemia, and minimally invasive robotic surgery for prostate cancer. He had no history of exposure to retinotoxic medications. He had bilateral cataract extractions with implantation of intraocular lenses in his early 40 s. The patient's family is of English ancestry with no family history of inherited retinal degenerations, blindness or known parental consanguinity. He has four adult children: two daughters and two sons, all visually asymptomatic.

On initial examination, best-corrected visual acuity was 20/20 in each eye. Slit lamp biomicroscopy showed centered posterior chamber intraocular lenses and rare stranded vitreous cells in both eyes. Fundus examination was notable for vascular attenuation and clumpy pigmentation in the periphery of both eyes, most obvious inferiorly (Fig. 1a). Color vision assessed with the Farnsworth D-15 panel was normal in both eyes.

Fluorescein angiography showed no vascular anomalies in both eyes (Supplementary Fig. 1). SW-FAF and NIR-FAF imaging demonstrated a preserved island of fundus autofluorescence centrally extending superiorly beyond the vascular arcades (Fig. 1b). A ring of hyperautofluorescence, most obvious on NIR-FAF (Fig. 1b, yellow arrows), separated the central area of normal-appearing autofluorescence from a well-defined peripheral boundary of hypoautofluorescence that allows visualization of the choroidal vasculature (Fig. 1b, white arrows). Kinetic visual fields measured with a V-4e and III-4e targets showed generalized constriction to $-40°$ of eccentricity inferiorly and a pseudo-altitudinal defect in both eyes (Fig. 1c). The two isopters are close to each other, while the field measured with the smallest (I-4e) target is constricted to $-10°$ of eccentricity in both eyes (Fig. 1c). Standard full-field ERGs showed clearly detectable but significantly reduced amplitudes (-10% of normal) of both rod- and cone-mediated responses (Fig. 1d).

Detailed retinal function was measured with light- and dark-adapted (two-color) automatic static perimetry (Fig. 2a). A sensitivity profile co-localized to the central SD-OCT cross sections showed near-normal light-adapted sensitivity near fixation and into nasal retina. Within the central 4 mm of eccentricity, light-adapted sensitivities were reduced by less than 0.5 log units (l.u.), whereas rod-mediated sensitivities were reduced by ≤ 1 l.u. (Fig. 2a). Sensitivities declined with increasing distance from the center becoming severely reduced (> 3 l.u. from the mean normal) from 6 to 8 mm from the foveal center (Fig. 2b). By SD-OCT there was normal lamination within a 2 mm region around the fovea (Fig. 2b). The ONL was normal-appearing within this region, corresponding with the area of better sensitivities measured with perimetry. The more peripheral retina beyond 2 mm showed normal lamination, but gradual ONL thinning and loss of the inner segment ellipsoid (EZ) and photoreceptor outer segment interdigitation (IZ) signals. The ONL thickness declined asymmetrically with eccentricity in both eyes, with greater loss noted in the temporal retina (Fig. 2b). This structural change was accompanied by diminished, nondetectable, or severely abnormal retinal sensitivity as noted on perimetry. Genetic testing revealed compound heterozygous variants (p.Arg567Ter (CGA > TGA); c.1699C > T and p.Leu566His (CTC > CAC); c.1697 T > A) in exon 5 of the *ZNF408* gene. The next-generation sequencing data indicated that the R567X and L566H variants are present on opposite *ZNF408* alleles (in trans) in this individual (Supplementary Fig. 2).
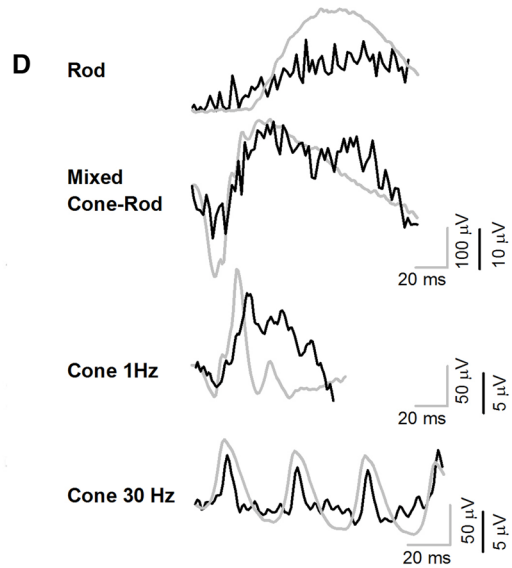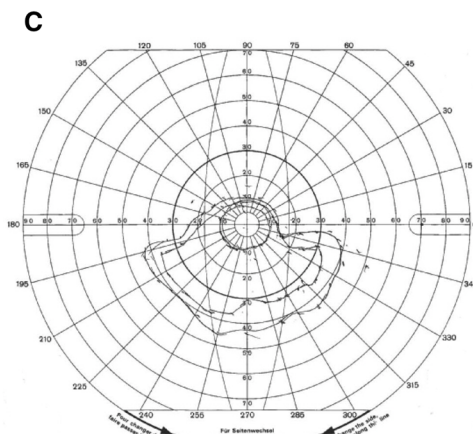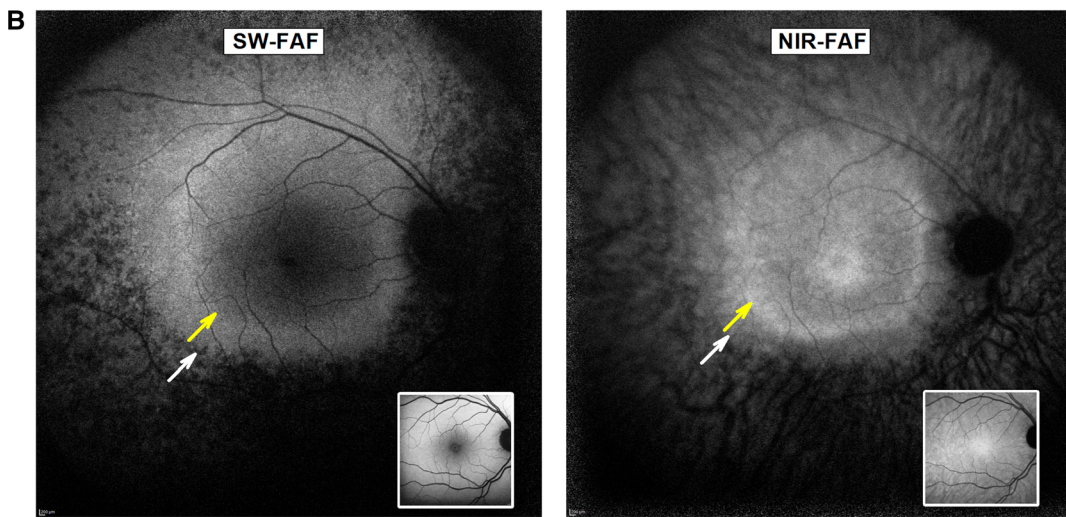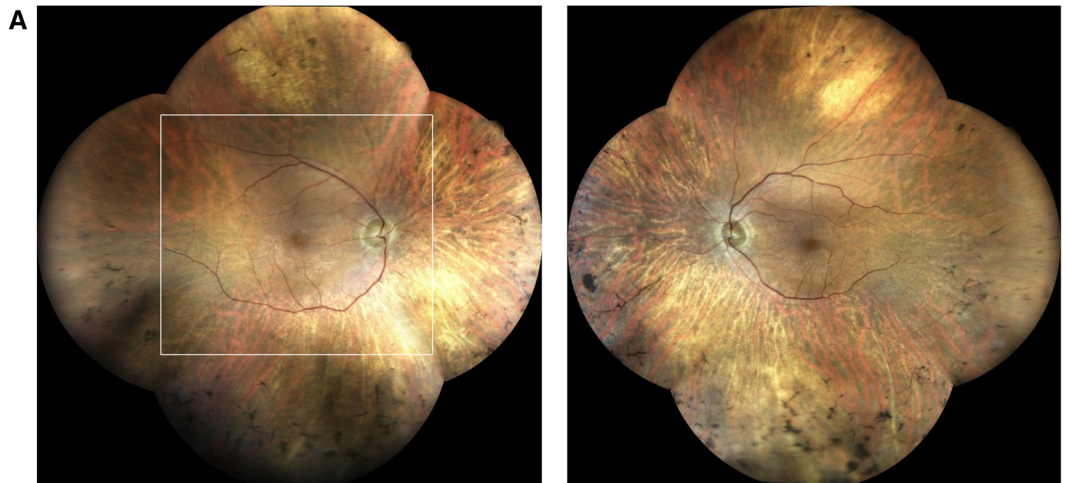
◀**Fig. 1** Retina-wide structure and function in the patient. **a** Wide-field color photomontage (102°) of both eyes. **b** Fundus autofluorescence (FAF) imaging elicited with short wavelength (SW-FAF) and near-infrared (NIR-FAF) from the central retina (30 degrees = white box) of the right eye. Arrows point to the boundary between the central region with normal FAF and the more peripheral retina with reduced FAF signal and visualization of the background choroidal vasculature (white arrows) as well as a faint, broad ring of hyperautofluorescence (yellow arrows). **c** Goldmann kinetic perimetry from the right eye. Shown are three isopters which represent, from peripheral to most central, Goldmann V-4e, III-4e and I-4e stimuli. **d** Full-field ERGs from the patient (black traces) compared to a representative normal subject (gray traces). Calibration bars are to the right and bottom of the traces; gray bars are scale bars for the normal subject which represent × 10 the amplitude of the patient (black vertical scale bars). Stimulus onset is at trace onset. For clarity, only right eye responses shown

Discussion

We present a detailed phenotype of a patient with variants in the *ZNF408* gene inherited in a compound heterozygous state. The associated disease was characterized by a late symptomatic onset (7th decade of life) of a pigmentary retinopathy that fits within the spectrum of RP, specifically, forms of this condition with relatively preserved, or even normal, central retinal structure and function, also reminiscent of *concentric* RP [22–24]. Our patient harbored a p.R567X variant in *ZNF408*, which has been previously reported segregating with RP in compound heterozygosity [25]. This variant causes a truncation of 154 amino acids predicted to cause loss of protein function [25]. The patient's second variant, p.L566H, is rare and previously unpublished. It is present in Gnomad in 1/244,176 alleles and results in a non-conservative amino acid substitution that is likely to impact secondary protein structure as the residues are distinct in polarity, charge, size and other properties. In silico analyses, including protein predictors and evolutionary conservation, also support a deleterious effect (Provean score − 6.83).

Exome sequencing, linkage and segregation analyses in large Norrie disease/FEVR pedigrees have led to the identification of several causative genes, including *LRP5, FZD4, TSPAN12, NDP, KIF11, CTNB1, ATOH7* and *ZNF408* [26–28]. More recently, whole exome sequencing has led to the identification of *ZNF408* mutations in families with arRP in two prior reports [13, 15]. Avila-Fernandez et al. described

two homozygous pathogenic variants in *ZNF408* associated with arRP with localized vitreous condensations in two unrelated Spanish families [13]. Patients presented with nyctalopia and visual field constriction and abnormally reduced or undetectable ERGs. Interestingly, two siblings from a family carrying a homozygous truncation mutations (p.Ala122Leufs*2) predicted to result in total loss-of-function of the protein, were diagnosed, like our patient, late in life, in their 50s. These two patients, and a third patient from an unrelated family with a missense mutation (p.Arg541Cys), enjoyed relatively preserved central vision (visual acuities > 0.6 decimal, > 20/30 in at least one eye) and had near-normal central retinal lamination by OCT at ages 50, 67 and 69, respectively. The second report by Habibi et al. documented on three sisters from a consanguineous Tunisian family in which homozygous splice site mutations (c.652-1G > T) in *ZNF408* segregated with arRP associated with vitreal opacities and moderately high myopia (− 6 to − 10D)[15]. While they had a similar but slightly earlier symptomatic onset (20–30 years of age), and their visual acuities were more affected when examined at ages 36–48 (0.2–0.5 decimal, 20/40–20/100), the documented OCTs in the patient with worse acuity still showed preserved ONL near the foveal center, despite the presence of an epiretinal membrane and associated trace cystoid edema, and were interpreted as 'normal patterns' in the other two sisters. There was no obvious progression in a 5-year follow-up. The detailed phenotype in our 70-year-old patient was remarkably similar with preserved retinal lamination, photoreceptors and RPE by multimodal imaging near the foveal center that gradually tapered in thickness with increasing eccentricity. Despite severely abnormal ERGs, our patient showed near-normal cone-mediated sensitivities near the center and relatively preserved rod function extending from − 20 to 25° from fixation, a pattern that resembles forms of RP with locally near normal or normal retina [9, 29]. Of note, none of the patients from this or the earlier studies showed obvious vascular abnormalities, although in these cases it is conceivable that subtle peripheral abnormalities may be obscured by the overlapping degeneration. The functional and structural phenotype suggests losses of vision following protracted photoreceptor loss without direct interference with their function, perhaps from loss of a
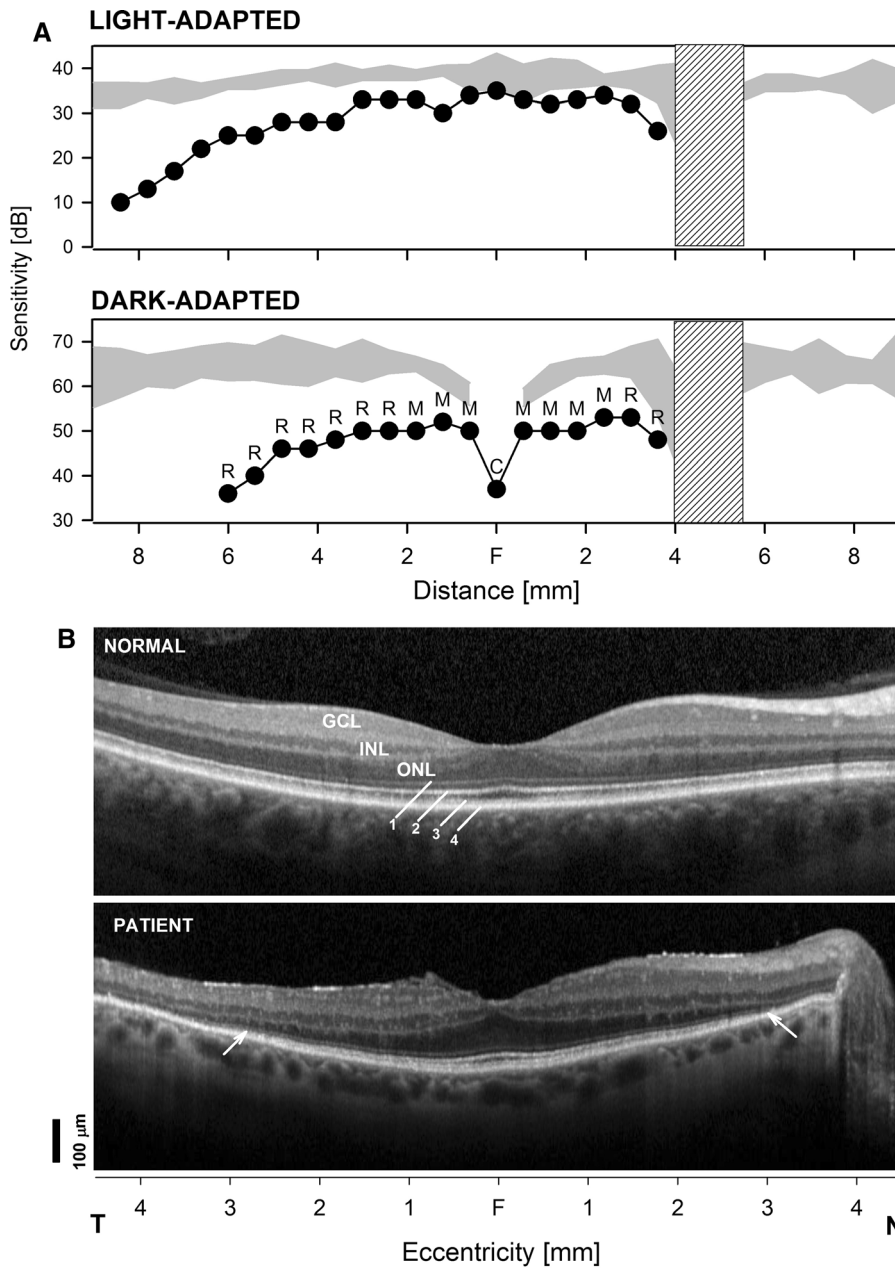
Fig. 2 a Horizontal sensitivity profile measured by automatic static perimetry in the patient obtained in the light- (achromatic stimulus) and dark-adapted state (500 nm stimulus) and compared to the normal range (gray band = mean ± 2SD). Photoreceptor mediation was estimated with two-color (650 nm and 500 nm) dark-adapted sensitivity differences and labeled as follows: M = mixed-mediated, R = rod-mediated, C = cone-mediated. Hatched bar: blind spot. **b** Shown are SD-OCT horizontal (9 mm-long) cross sections through the fovea in the patient compared to a representative normal subject (**a**), and from the fovea into nasal retina (**b**) in the patient. Nuclear layers are labeled: outer nuclear layer = ONL, inner nuclear layer = INL, ganglion cell layer = GCL. OPL = outer plexiform layer; ELM = external limiting membrane. Outer retinal laminae are labeled with diagonal arrows: 1. OLM, outer limited membrane, 2. inner segment ellipsoid band (EZ), 3. photoreceptor outer segment tip to apical RPE interdigitation, 4. RPE/BrM. Arrows in the patient delineate segments with detectable laminations sclerad to the ONL in the outer retina. Arrows point to transitional zone where the EZ approaches the apical RPE and become non-discernible. T = temporal, N = nasal, F = Fovea

putative photoreceptor maintenance function of ZNF408 [13].

At this point it is still unclear why certain FEVR-causing genetic variants, including ZNF408 mutations, would lead to such apparently distant phenotypes and whether a connection between the different underlying diverse disease mechanisms exists. Specifically, the FEVR phenotype, while of somber prognosis due to the frequency and severity of complications emerging from the abnormal retinal vascularization, does not carry a retinal degeneration component. The reported arRP cases and the chorioretinopathies associated with *KIF11*, for example, imply a post-developmental degenerative component superimposed to the developmental problem with a spectrum ranging from predominantly developmental disease to one dominated by the degeneration. ZNF408 variants associated with arRP include both loss-of-function and missense (Y524X, c.363_364delTG/p.Ala122Leufs*2, c.653-1G > T/IVS4-1G > T, R541C, R448C) mutations. Our study proposes additional missense mutations near the location within the protein of at least one of the earlier reports of *ZNF408*-arRP [13]. ZNF408 comprises 10 of C2H2-type zinc finger domains that could have different and still unknown cellular functions. Mutations in different domains may alter the interaction of ZNF408 with specific targets and result in specific phenotypes, such as arRP. Further studies are needed to confirm our findings and the role that the specific mutations reported herein have in the pathophysiology of this specific phenotype. The introduction of FEVR genes in comprehensive, commercially available, gene screening panels for IRDs may lead, despite the perceived low prevalence of this genotype and associated RP phenotype, to the identification of new mutations and/or FEVR genes in retinopathies that do not clinically conform to FEVR.

Declarations

Conflict of interest No conflict of interest related to this work for any of the authors. Jane Juusola is an employee of GeneDx.

Informed Consent The patient has consented to the submission of the case report to the journal.

Statement of human rights This is a retrospective review of the clinical record of a patient seen as part of his standard of care. The visit adhered to HIPAA regulations, the patient offered informed consent to the diagnostic procedures and all personal identifiers have been removed. All procedures were performed in accordance with the ethical standards of involved institutions and with the Declaration of Helsinki.

Statement on the welfare of animals This manuscript does not contain any studies with animals.

References

1. Fahim AT, Daiger SP, Weleber RG (1993) Nonsyndromic retinitis pigmentosa Overview. In: Adam MP, Ardinger HH, Pagon RA, Wallace SE, Bean LJH, Stephens K, et al. (edrs.) GeneReviews((R)). Seattle (WA)
2. Hartong D, Berson E, Dryja T (2006) Retinitis pigmentosa. Lancet 368(9549):1795–1809
3. Verbakel SK, van Huet RAC, Boon CJF, den Hollander AI, Collin RWJ, Klaver CCW et al (2018) Non-syndromic retinitis pigmentosa. Prog Retin Eye Res 66:157–186. https://doi.org/10.1016/j.preteyeres.2018.03.005
4. Berson EL (1993) Retinitis pigmentosa. Invest Ophthalmol Vis Sci 34(5):1659–1676
5. Berson EL (1976) Retinitis pigmentosa and allied retinal diseases: electrophysiologic findings. Trans Sect Ophthalmol Am Acad Ophthalmol Otolaryngol. 81(4 Pt 1):OP659–OP666
6. Berson EL (1993) Retinitis pigmentosa: The Friedenwald Lecture. Invest Ophthalmol Vis Sci. 34(5):1659–1676
7. Berson EL (2007) Long-term visual prognoses in patients with retinitis pigmentosa: the Ludwig von Sallmann lecture. Exp Eye Res 85(1):7–14. https://doi.org/10.1016/j.exer.2007.03.001
8. Jacobson S, Voigt W, Parel J-M, Apathy P, Nghiem-Phu L, Myers S et al (1986) Automated light- and dark-adapted perimetry for evaluating retinitis pigmentosa. Ophthalmology 93:1604–1611
9. Jacobson SG, Roman AJ, Aleman TS, Sumaroka A, Herrera W, Windsor EA et al (2010) Normal central retinal function and structure preserved in retinitis pigmentosa. Inv Ophthalmol Vis Sci 51(2):1079–1085. https://doi.org/10.1167/iovs.09-4372
10. Bhatti MT (2006) Retinitis pigmentosa, pigmentary retinopathies, and neurologic diseases. Curr Neurol Neurosci Rep 6(5):403–413. https://doi.org/10.1007/s11910-996-0021-z
11. Criswick VG, Schepens CL (1969) Familial exudative vitreoretinopathy. Am J Ophthalmol 68(4):578–594. https://doi.org/10.1016/0002-9394(69)91237-9
12. Benson WE (1995) Familial exudative vitreoretinopathy. Trans Am Ophthalmol Soc 93:473–521

13. Avila-Fernandez A, Perez-Carro R, Corton M, Lopez-Molina MI, Campello L, Garanto A et al (2015) Whole-exome sequencing reveals ZNF408 as a new gene associated with autosomal recessive retinitis pigmentosa with vitreal alterations. Hum Mol Genet 24(14):4037–4048. https://doi.org/10.1093/hmg/ddv140

14. Gilmour DF (2015) Familial exudative vitreoretinopathy and related retinopathies. Eye 29(1):1–14. https://doi.org/10.1038/eye.2014.70

15. Habibi I, Chebil A, Kort F, Schorderet DF, El Matri L (2017) Exome sequencing confirms ZNF408 mutations as a cause of familial retinitis pigmentosa. Ophthalmic Genet 38(5):494–497. https://doi.org/10.1080/13816810.2016.1275020

16. Shurygina MF, Simonett JM, Parker MA, Mitchell A, Grigorian F, Lifton J et al (2020) Genotype phenotype correlation and variability in microcephaly associated with chorioretinopathy or familial exudative vitreoretinopathy. Inv Opthalmol Vis Sci 61(13):2. https://doi.org/10.1167/iovs.61.13.2

17. Collin RW, Nikopoulos K, Dona M, Gilissen C, Hoischen A, Boonstra FN et al (2013) ZNF408 is mutated in familial exudative vitreoretinopathy and is crucial for the development of zebrafish retinal vasculature. Proc Natl Acad Sci U S A 110(24):9856–9861. https://doi.org/10.1073/pnas.1220864110

18. Karjosukarso DW, Ali Z, Peters TA, Zhang JQC, Hoogendoorn ADM, Garanto A et al (2020) Modeling ZNF408-associated FEVR in zebrafish results in abnormal retinal vasculature. Inv Ophthalmol Vis Sci 61(2):39. https://doi.org/10.1167/iovs.61.2.39

19. Aleman T, Morgan J, Serrano L, Han H, Fuerst N, Charlson E et al (2017) Natural history of the central structural abnormalities in choroideremia: a prospective cross-sectional study. Ophthalmology 124:359–373

20. McCulloch DL, Kondo M, Hamilton R, Lachapelle P, Messias AMV, Robson AG et al (2019) ISCEV extended protocol for the stimulus-response series for light-adapted full-field ERG. Doc Ophthalmol 138(3):205–215. https://doi.org/10.1007/s10633-019-09685-8

21. Retterer K, Juusola J, Cho MT, Vitazka P, Millan F, Gibellini F et al (2016) Clinical application of whole-exome sequencing across clinical indications. Genet Med 18(7):696–704. https://doi.org/10.1038/gim.2015.148

22. Farber MD, Fishman GA, Weiss RA (1985) Autosomal dominantly inherited retinitis pigmentosa: visual acuity loss by subtype. Arch Ophthalmol 103(4):524–528. https://doi.org/10.1001/archopht.1985.01050040066019

23. Grover S, Fishman GA, Brown J Jr (1998) Patterns of visual field progression in patients with retinitis pigmentosa. Ophthalmology 105(6):1069–1075. https://doi.org/10.1016/S0161-6420(98)96009-2

24. Milam AH, De Castro EB, Smith JE, Tang W-X, John SK, Gorin MB et al (2001) Concentric retinitis pigmentosa: clinicopathologic correlations. Exp Eye Res 73(4):493–508. https://doi.org/10.1006/exer.2001.1059

25. Stone EM, Andorf JL, Whitmore SS, DeLuca AP, Giacalone JC, Streb LM et al (2017) Clinically focused molecular investigation of 1000 consecutive families with inherited retinal disease. Ophthalmology 124(9):1314–1331. https://doi.org/10.1016/j.ophtha.2017.04.008

26. Li Y, Peng J, Li J, Zhang Q, Li J, Zhang X et al (2018) The characteristics of digenic familial exudative vitreoretinopathy. Graefes Arch Clin Exp Ophthalmol 256(11):2149–2156. https://doi.org/10.1007/s00417-018-4076-8

27. Li JK, Li Y, Zhang X, Chen CL, Rao YQ, Fei P et al (2018) Spectrum of Variants in 389 Chinese probands with familial exudative vitreoretinopathy. Inv Ophthalmol Vis Sci 59(13):5368–5381. https://doi.org/10.1167/iovs.17-23541

28. Wang S, Zhang X, Hu Y, Fei P, Xu Y, Peng J et al (2021) Clinical and genetical features of probands and affected family members with familial exudative vitreoretinopathy in a large Chinese cohort. Br J Ophthalmol 105(1):83–86. https://doi.org/10.1136/bjophthalmol-2019-315598

29. Aleman TS, Cideciyan AV, Sumaroka A, Windsor EA, Herrera W, White DA et al (2008) Retinal laminar architecture in human retinitis pigmentosa caused by Rhodopsin gene mutations. Inv Ophthalmol Vis Sci 49(4):1580–1590. https://doi.org/10.1167/iovs.07-1110